PAPER • OPEN ACCESS

Resolving XUV induced femtosecond and attosecond dynamics in polyatomic molecules with a compact attosecond beamline

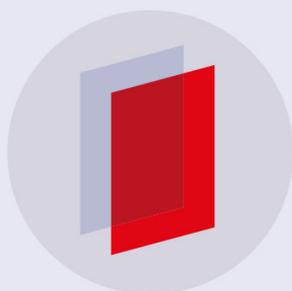To cite this article: V Loriot *et al* 2015 *J. Phys.: Conf. Ser.* **635** 012006

View the article online for updates and enhancements.

Related content

Recent citations

IOP ebooks™

Bringing you innovative digital publishing with leading voices to create your essential collection of books in STEM research.

Start exploring the collection - download the first chapter of every title for free.

Resolving XUV induced femtosecond and attosecond dynamics in polyatomic molecules with a compact attosecond beamline

V. Loriot[1], **A. Marciniak**[1], **L. Quintard**[2], **V. Despré**[1], **B. Schindler**[1], **I. Compagnon**[1,3], **B. Concina**[1], **G. Celep**[1], **C. Bordas**[1], **F. Catoire**[2], **E. Constant**[2] **and F. Lépine**[1]

[1] Institut lumière matière, UMR5306 Université Claude Bernard Lyon 1-CNRS, Université de Lyon 69622 Villeurbanne cedex, France
[2] Univ. Bordeaux, CEA, CNRS, CELIA, UMR5107, F-33400 Talence, France
[3] Institut Universitaire de France IUF, 103 Blvd St. Michel, 75005 Paris, France

E-mail: Franck.Lepine@univ-lyon1.fr

Abstract. XUV induced dynamics in molecules is still largely unexplored while experimental and theoretical tools are becoming available in several labs. In this work, we present a compact XUV beamline designed to induce and probe femtosecond and attosecond dynamics in gas samples (from atoms to complex molecular species). The induced processes are studied with time-resolved photoelectron or/and photoion imaging. The characterization of the performances of the experimental setup is presented. We show experimental results obtained in naphthalene molecule showing femtosecond and attosecond time-resolved photoelectron imaging experiments allowing electron wavepacket phase measurements.

1. Introduction

Attoscience is a rapidly expanding field of research that explores physical processes associated with electron dynamics in atoms, molecules and surfaces [1]. High Harmonic Generation (HHG) process used to synthesize attosecond pulses can, by itself, be exploited to extract physical properties of matter due to its sensitivity to nuclear and hole dynamics, orbital shapes or chirality [2]. By choosing the HHG conditions and using adapted XUV optics, polarization [3], spatial and spectral, amplitude, and phase of the harmonics can be controlled [4]. Nowadays such controlled attosecond pulses are exploited in pump-probe schemes with a delayed infrared pulse, reaching attosecond temporal resolution. The attosecond pulse can be used either as a pump or as a probe to investigate molecular species [5]. XUV photons in attosecond pulses have enough energy to one-photon ionize most of the atomic or molecular species. This ionization step can be used as a probe where the analysis of the resulting photoelectrons provides rich information on the atomic or molecular states involved in the dynamics at a given time. On the other hand, the XUV pulse can also be used as a pump since the ionization can trigger dynamical processes by creating non-stationnary states. The first ever molecular attosecond pump-probe experiment was dealing with photo-dissociative ionization and attosecond charge localization in the most simple molecule: H_2 [6]. Soon afterward, attosecond control of fragmentation processes have been performed in H_2 [7] and in O_2 [8] using attosecond interferometric schemes. Attosecond

XUV-IR pump-probe experiments in molecules have been extended to slightly larger species, in experiments where the total molecular ionization rate was modulated on the attosecond timescale in N_2, CO_2 and C_2H_4 [9]. C_2H_4 is so far, the most complex system that has shown attosecond dynamics in pump-probe configuration. In recent investigations, the extension to larger molecular species have been illustrated in experiments where few femtosecond dynamics could be observed in phenylalanine [10, 11] and attosecond photoemisison delay could bring information on plasmon resonance in C_{60} [12]. In a polyatomic molecule, the ionization of an inner valence electron can let the cation in an excited state. For high energy photons, electron correlation can play a major role in defining the states involved, and following the ionization step, non-adiabatic relaxation can drive the time dependent evolution of the system. Such XUV induced processes are of a high interest and open the way to the investigation of unexplored mechanisms such as charge migration [13]. Due to the complexity of the mechanisms involved in ultrashort time scale dynamics in molecules, sophisticated spectroscopic techniques and highly reliable beamlines are required.

In this paper, we present a compact atto-femtosecond XUV-IR beamline specially designed to investigate the dynamics on the attosecond and femtosecond time scale in molecules. The attosecond pulse train (APT) is characterized using an homemade XUV spectrometer, and its temporal characteristics are reconstructed with a standard Attosecond Beating By Interference of Two photon Transition (RABBITT) method [14]. Then, we show the first results obtained on a large molecule (naphthalene, $C_{10}H_8$) where the response is expected to be more complex than the atomic case due to the richness of the electronic structure. XUV induced excitation followed by non-adiabatic relaxation on the femtosecond timescale is observed by measuring the time-resolved di-cation yield. On the attosecond timescale, phase variations of the molecular photoelectron wavepackets are measured showing variations across the $\sigma \to \sigma^\star$ resonance. The photoelectron spectrum is interpreted using the Algebraic Diagrammatic Construction (ADC) [15] method that explicitly takes into account multielectronic effects.

2. Method
2.1. Experimental setup
Several configurations of XUV-IR beamlines can be found in the literature [16–19]. Here we propose a compact solution based on the implementation of a setup proposed in Cabasse *et al.* [20] and Driever *et al.* [21]. The pump-probe configuration developed here is shown in figure 1. It is composed by a long interferometer placed on an independent optical table (where the XUV up-conversion is realized in one arm) seeded by 25 fs long pulses at $\lambda_0 \approx 807$ nm, 2 mJ with 5 kHz repetition rate delivered by a commercial amplifier laser system (Coherent elite duo USX) coupled to a Velocity Map Imaging (VMI) spectrometer.

The incoming laser beam is split in two parts at the entrance of the optical table and the transmitted part is up-converted through HHG process into XUV photons by focusing the fundamental beam with a refractive lens (30 cm focal length) into a 3 mm windows-less static gas cell [22] filled by a noble gas (Krypton or Xenon). The pressure is maintained at tens of mbar into the cell while the background pressure of the chamber is kept below 10^{-4} mbar. The interaction with the gas produces High Harmonics (HH) collinearly to the fundamental beam that is filtered at the entrance of the recombination chamber using an XUV beam splitter treated in transmission for 800 nm. The beamsplitter is coated with Nb_2O_5 that has a good reflectivity ($\approx 45\%$) for XUV radiation at grazing angle ($\approx 68°$). The XUV beam divergence is controlled by a 30 cm focal length toroidal gold mirror that focuses the harmonics into the VMI interaction region. A 200 nm aluminum filter can be positioned after the toroidal mirror in order to remove the residual IR light, and also to compress the harmonics and compensate the attochirp [4]. The XUV beam is then reflected by a planar gold grating placed on a motorized rotation stage used at the zero order for experiments and at the first order diffraction to measure the XUV
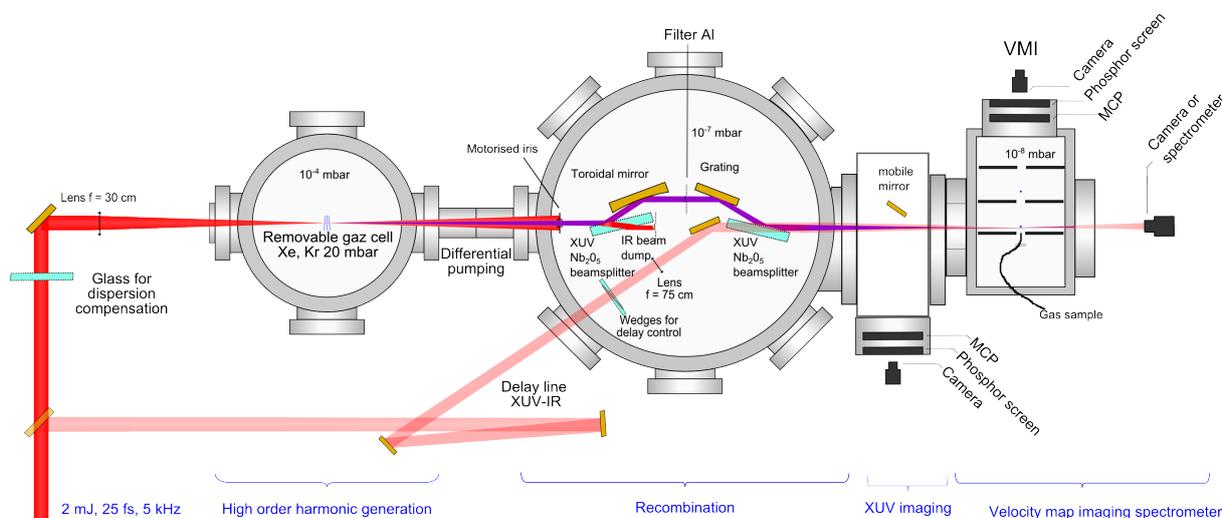
Figure 1. Experimental setup.

spectrum. The APT is then recombined with the other arm (time delayed IR pulse of 25 fs) by another Nb_2O_5 coated XUV beamspliter.

The stability of the overall setup is estimated by measuring the spectral interference of an IR beam that propagates through both arms of the interferometer with a delay of few hundreds of femtoseconds (figure 2(a)). Measuring the phase of the spectral interference over an hour
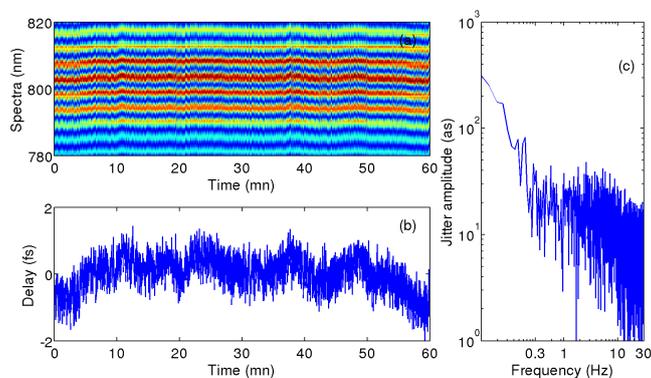

Figure 2. (a) Measurement of the stability of the interferometer using the spectral interference at 800 nm integrating over 0.2 ms (single shot) (b) its corresponding delay drift and (c) the Fourier transform of this last.

(figure 2b), a delay drift of 535 as rms can be extracted that is mainly due to the slow fluctuations as shown by the Fourier transform analysis of the signal (figure 2c), below 380 as rms is measured over a minute.

The time delay between the APT and the IR pulse is controlled by a refractive delay line on the IR arm composed by a motorized 4° wedge pair (WP) that is equivalent to a piece of glass with a variable thickness. According to the link between the pulse duration and the chirp introduced by the dispersion, a spreading of the pulse from 25 to 26 fs would require a dispersion of about ± 65 fs^2, it means that, when the incoming pulse is initially unchirped, the pulse duration can be considered insensitive to the dispersion over a range of 130 fs^2. Considering the fuse silica dispersion around 800 nm of 36 fs^2/mm, a glass insertion of 3.6 mm would not significantly affect the pulse duration while it represents a time-delay range of 6.5 ps. The refractive delay line is hence very well suited for attosecond and femtosecond delay scan using pulses of tens of femtoseconds.

The APT and IR beams are recombined and then focused with respectively TG and L_2 into a VMI spectrometer optimized to work with a dense atomic or molecular source by injecting the atomic/molecular jet directly through the repeller electrode [23].

2.2. Characterization of the attosecond pulse train

The XUV spectrum corresponding to the APT is measured at the first order of diffraction of the gold grating (600 grooves/mm) [20, 21]. For that purpose, the XUV beam is reflected by inserting a gold mirror at 45° incidence angle (see GM figure 1) and sent to a MCP-phosphor assembly. To obtain the full spectrum, the grating is rotated over 3-4° with small steps (typically 0.05°) to prevent any inhomogeneity in the detection. Figure 3 shows the 2D resolved harmonic
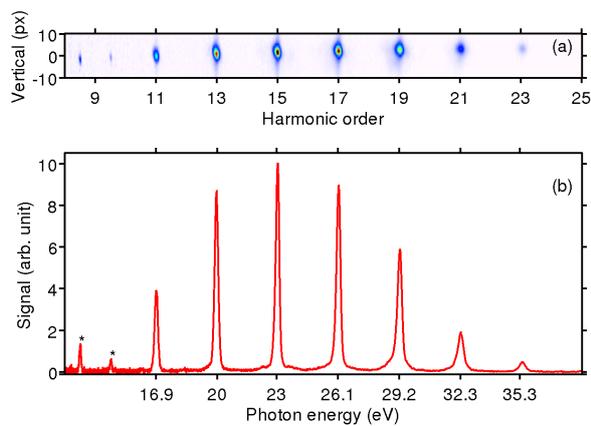

Figure 3. *(a)* HHG spectra generated in Xenon measured by the XUV imaging system (see figure 1) placed on the focal plan of the toroidal mirror (TG) and *(b)* its corresponding integration over the vertical coordinate considering the fundamental wavelength of 807 nm. $(\star)$ is the 2nd order of diffraction.

spectrum generated in xenon at the focus, and its corresponding XUV spectrum obtained by integrating the signal over the vertical coordinate assuming that the spatial profile does not limit the spectral resolution. The spectrum is composed of a comb of peaks separated by $\approx$ 3 eV with a Gaussian envelop centered around 23.5 eV with 12 eV FWHM that can support 200 as pulses. This spectrum slightly differs from an usual plateau-like harmonics because of the 200 nm Aluminum filter and the 4 accumulated XUV reflective optics in the optical path.

The temporal profile of the APT is reconstructed through RABBITT measurements [14, 17, 24, 25] using a VMI spectrometer (see figure 4). The RABBITT proceeds as follows:
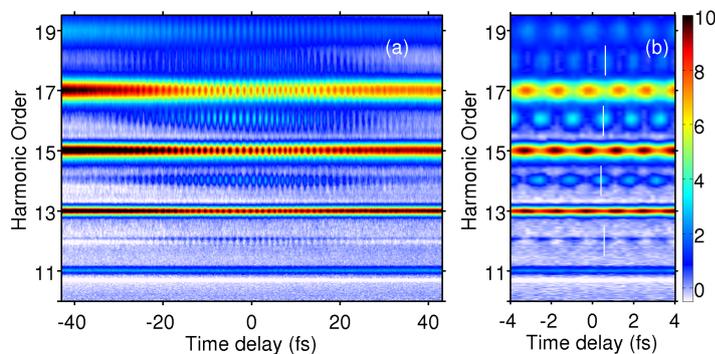

Figure 4. Typical RAB-BITT measurement in Argon over a *(a)* a temporal range that cover the full cross-correlation and *(b)* a zoom on the central part. the sidebands maximums are indicated by solid white lines.

photoelectron velocity distribution is measured at several delays between the IR and XUV pulses with attosecond precision over 80 fs (zero delay corresponds to IR -XUV time overlap). At a given delay the photoelectron image is angularly integrated leading to a photoelectron

kinetic energy spectrum. Thanks to a dense gas jet in the interaction region of the VMI, a relatively high photon flux and the 5 kHz repetition rate, only few seconds integration time is required per image, hence the full temporal overlap scan (figure 4a) requires tipically ten minutes of acquisition time. Such measurements are performed without any active stabilization tool thanks to the intrinsic stability of the beamline. The kinetic energy spectrum is composed of the electron signal given by each harmonic (the electron signal from harmonic order 11, 13, 15, 17 an 19 are seen in the figure 4b), and so-called sidebands in between that correspond to electrons produced via the absorption of an harmonic plus one IR photon. Figure 4(b) reveals that the maximum signal intensity of the sidebands is reached at almost the same time-delay ($\pm$ 100 as) indicating a quasi flat spectral phase of the harmonics hence a reasonably good compression of the attosecond pulse train.

3. Result obtained on Naphthalene target

3.1. Introduction
Photoionization is one major output of the absorption of an XUV photon by a complex molecule. Electron ejection can occur from several possible molecular orbitals, and consequently, for a neutral species, the remaining cation can be left in several possible electronically excited states. From this initial excitation step, a variety of mechanisms can occur such as charge dynamics, internal energy conversion through ro-vibration states or dissociation. The use of an APT composed of several photon energies to trigger these dynamics increase the complexity of the initiated dynamics. Probing such XUV induced mechanisms by a delayed femtosecond IR pulse is also a delicate step because many processes can be entangled. So far, only few experiments have been performed using ultrafast XUV/IR pump-probe spectroscopy on complex molecules due to the difficulty of disentangling the mechanisms [10,11,26] and it is crucial to isolate specific targets for which such measurement is accessible. One aspect that makes the understanding of the dynamics more accessible is the investigation of stable molecular species where no fragmentation occurs. Indeed in that case, the problem to address is limited to stable molecular structures which simplifies the implementation of a theoretical model.

Recently, we have investigated the XUV induced ultrafast non-adiabatic relaxation in polycyclic aromatic hydrocarbon (PAH) molecules. In this experiment the time dependent variation of the dication yield was measured as a function of the delay between the XUV and IR pulse [26]. In this experiment, the relaxation lifetime of excited cations produced by the XUV light has been probed. It was found that the relaxation timescale remained unchanged when tuning the pump XUV spectrum (by changing the HHG gas) and the probe IR intensity. In the present experiment, this robustness of the measured lifetime with respect to the laser parameters has been studied by reproducing this result with the setup presented above. A few differences exist in this new experiment compared to our previous investigations : the central wavelength of the laser seed is higher (λ_0=807 nm instead of 800 nm) and the pulse is shorter (25 fs instead of 35 fs). The experimental result and its fit is presented in Fig. 5. As in our pioneer work, the
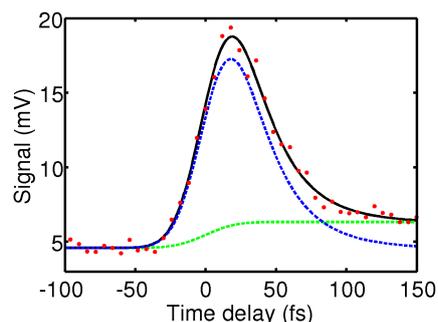
Figure 5. Time resolved ionization yield of the dication of Naphthalene (red dot) and its corresponding fit (black solid line) composed by two contributions that are the exponential decay corresponding to the non-adiabatic relaxation (blue dash line) and a step function that illustrate the amount of population trapped in an excited state (green dot line).

dynamics was composed by two contributions *(i)* an ultrafast decay and *(ii)* a step function. Both are convoluted by the cross-correlation for the two (IR and XUV) pulses that determines the temporal resolution. The decay can be explained as follows : the molecule absorbs a single XUV photon that ejects an electron while leaving the molecule in excited states. For this photon energy, the resulting state is strongly determined by electron correlation. As a result, single holes and shake-up states are created. Shake-up states correspond to situations where the electron ejection is accompanied by the promotion of a second electron to an excited state. This is a typical signature of multielectronic effects in photoionization. The resulting excited cation can be further ionized by the IR probe while it is in a state of high enough energy. Nevertheless the non-adiabatic couplings between electronic states lead to an ultrafast relaxation from one state to another releasing the energy into vibrational degrees of freedom. The relaxation proceeds up to a point where the accessed electronic state is energetically low enough that the IR probe can not ionize the molecule anymore. Note that the step function represents a part of the excited cationic population that is trapped in an excited states for which the relaxation process takes place on a much longer timescale.

The measurement with our new experimental setup provides a decay of 28 fs (with a cross-correlation of 35 fs) that fully matches our previous result of (29.4 ± 4) fs [26]. This last experimental result supports the previous conclusion of an ultrafast decay insensitive to laser conditions. However, the dication yield represents a very small fraction of the total amount of ionized species induced by the two color (XUV+IR) interaction. A more global view of the ionization step is given by studying the photoelectron spectrum as described in the following section.

3.2. Theoretical photoelectron spectra

The experimental photoelectron spectrum of naphthalene measured for a given XUV photon energy shows energetically localized structures allowing to identify the individual contributions from the Algebraic Diagrammatic Construction ADC(3) Green's function method [15]. The ADC calculation for the naphthalene ground state is presented in figure 6. Its 48 valence electrons lead to a rich structure that is interestingly grouped in broad bands spaced by about 3 eV.
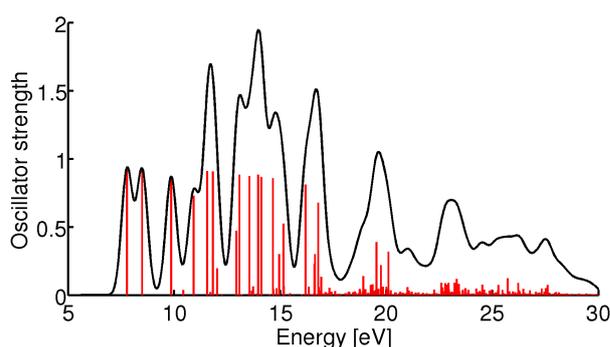

Figure 6. ADC spectra of naphthalene in the ground state (vertical red bar) and its convolution with a Gaussian of 0.6 eV FWHM (solid black line).

The photoelectron pattern of naphthalene in XUV+IR experiment is expected to be even more complex. The molecule is excited with a comb of XUV frequencies then each photon energy produces its own pattern and these several contributions overlap. All the states that have a binding energy below the photon energy may appear in the photoelectron spectra. Moreover, the IR pulse increases the degree of complexity of the observed photoelectron spectrum since it opens new channels and the IR photon can redistribute the photoelectron oscillator strength in the spectra.

3.3. Time resolved photoelectron spectra

Based on the previous theoretical prediction, one might expect that the complexity of the electron spectrum would lead to a complete loss of information and no signature of the molecular property in the time-dependent electron signal. To test this intuition, we perform this experiment with femtosecond and attosecond resolution (see figure 7) focussing our attention on high energy electrons. On the femtosecond timescale, multiple scans (several scan over the same temporal
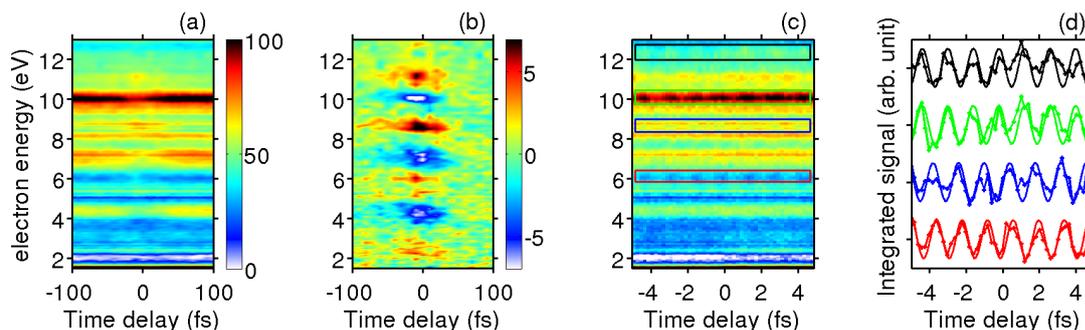

Figure 7. Time resolved photoelectron spectra of Naphthalene (XUV+IR) on the *(a)* femtosecond and on the *(c)* attosecond time scale. The modulation of the distribution of the map *(a)* is presented in *(b)* removing the static signal. The modulation of the distribution on the attosecond time scale is presented in *(d)* integrating a set of energetic range (indicated by rectangle of corresponding color in map *(c)*).

windows averaged) has been performed to get the global photoelectron response around the overlap. The resulting time-resolved photoelectron spectra are presented in figure 7(a). A complex energy dependent pattern is observed showing distinguishable contributions every 3 eV (at 12 eV, 9 eV etc ...). This structure simply corresponds to the energy periodicity of the XUV comb. Around zero delay, part of the electron spectrum is enhanced or depleted over few tens of fs. The duration of the modulation corresponds to the cross-correlation between the IR and the APT pulses. This effect is easily observed by subtracting the signal obtained at long delays (figure 7(b)). By increasing the temporal resolution, a scan focused on 10 fs time window has been performed and is shown in figure 7-(c). Here we observe oscillations of the signal at specific photoelectron energies with a period of 1.33 fs. This is more pronounced by integrating the contribution of each photoelectron energy band over 0.5 eV (see figure 7(d)). The amplitude of the oscillations on the attosecond time scale does not follow the amplitude of the modulation on the femtosecond time scale. Moreover, we note that the relative phase ϕ between the oscillations presented in figure 7(d) evolves with the photoelectron energy as illustrated by the set of energetically integrated contributions. This energy dependent phase effect is higher than the one found in the case of RABBITT measurements in rare gases presented in section 2.2. This indicates that the phase measured is associated with the molecular photoionization process and not associated with the intrinsic attochirp of the harmonics.

3.4. Discussion

Despite the number of electronic states involved, different XUV photon energies and complexity added by the IR pulse, the time-resolved photoelectron distribution is rather simple. This relatively simple pattern is understood as follows.

   Along the electron kinetic energy axis the distribution is rather simple due to the periodicity of the frequency comb combined with the distribution of electronic states grouped as described in

the previous section (see figure 6). Moreover, the HHs do not equally contribute to the resulting photoelectron spectrum. The absorption cross-section has a maximum around 16 eV [27] that is at the edge of the XUV spectrum used in the experiment (see figure 3). Hence, only the few lowest harmonics significantly contribute to the spectrum that strongly simplifies the photoelectron distribution allowing to estimate the group of orbitals that are important in the experiment. The IR pulse does not introduce much more complexity to the distribution because, the intensity has been limited to induce single IR photon absorption. Therefore only first order sideband signal can be created.

Some specific kinetic energies present an oscillation with a period of 1.33 fs. The phases of the oscillations strongly depend on the photoelectron energy considered. The oscillation at twice the carrier frequency can be understood in terms of interferences between quantum paths that produce an electron at the same kinetic energy (see RABBITT experiments figure 4). The RABBITT method applied to atomic target is simpler because only few electronic state are usually involved and the sideband phase depends on the atomic phase and the attochirp of the APT. In our case the attochirp is quite small (figure 4(b)) hence the beating phases are significantly affected by the molecular phases.

The molecular phases are related to the molecular orbitals and therefore can strongly change as a function of the orbital that is considered. However, in the experiment, the energy resolution is not high enough to isolate photoelectron sidebands for a given molecular orbital, only a group of states (overlapped contributions) are measured. There is no reason why the group of states would lead to any distinguishable phase. Nevertheless, clear oscillations appear at some specific kinetic energies. This means that the states that are probed lead a global phase effect that we can distinguish in our experiment. In this photon energy range, it is known that the photoexcitation signal in naphthalene is dominated by $\sigma \rightarrow \sigma^\star$ transitions that correspond to excitation of in-plane orbitals, with the XUV light polarization parallel to the the molecular backbone. The phase measured will be related to the phase of the electron wavepacket ejected from such orbitals. Based on similar work performed on atomic targets [28], and with the concept of Wigner time delay, it is expected that the phase variation will be related to variations of the photoemission time delay across the large σ resonance. Such effect has been predicted in the very similar case of broad plasmon resonance of C_{60} molecules [12], and variation of photoemission delays were attributed to the role of electron correlation that is prominent at this photon energy. Further investigations will be presented in a coming article.

4. Conclusion

We have developed a new compact, robust and versatile experimental setup to measure XUV induced dynamics in complex molecules with femtosecond and attosecond resolution without any active stabilization of the delay line. The spectral characteristics of the XUV pulse are measured with a home-made XUV spectrometer while its temporal shape shows attosecond structure. The principal observables such as time-of-flight, photoelectrons and photoions velocity distribution are used to perform measurements as a function of time delay between the IR and XUV pulses. Ultrafast XUV induced non-adiabatic relaxation dynamics in naphthalene has been measured and the extracted decay time perfectly matches our previous measurements despite the different laser parameters used in this experiment. The time-resolved XUV/IR photoelectron spectra of naphthalene provides a simpler structure than expected allowing to obtain attosecond resolved photoelectron imaging measurements that show clear evidence for attosecond oscillations with phases related to the molecular properties. These effects are measured for the first time in such complex molecular target. Further investigations are on going.

Acknowledgments

References

[1] Krausz F and Ivanov M 2009 *Rev. Mod. Phys.* **81** 163–234
[2] Haessler S, Caillat J and Salières P 2011 *J. Phys. B* **44** 203001
[3] Ferré A *et al.* 2015 *Nat. Photonics* **8** 93
[4] López-Martens R *et al.* 2005 *Phys. Rev. Lett.* **94**(3) 033001
[5] Lépine F, Ivanov M Y and Vrakking M J J 2014 *Nat. Photonics* **8** 195–204
[6] Sansone G *et al.* 2010 *Nature* **465** 763–766
[7] Kelkensberg F *et al.* 2011 *Phys. Rev. Lett.* **107** 043002
[8] Siu W *et al.* 2011 *Phys. Rev. A* **84** 063412
[9] Neidel C *et al.* 2013 *Phys. Rev. Lett.* **111**(3) 033001
[10] Calegari F *et al.* 2014 *Science* **346** 336–339
[11] Belshaw L *et al.* 2012 *J. Phys. Chem. Lett.* **3** 3751–3754
[12] Barillot T *et al.* 2015 *Phys. Rev. A* **91**(3) 033413
[13] Kuleff A I, Lünnemann S and Cederbaum L S 2013 *Chem. Phys.* **414** 100 – 105
[14] Paul P M *et al.* 2001 *Science* **292** 1689–1692
[15] Deleuze M S, Trofimov A B and Cederbaum L S 2001 *J. Chem. Phys.* **115** 5859–5882
[16] Frank F *et al.* 2012 *Rev. Sci. Instr.* **83** 071101
[17] Locher R *et al.* 2014 *Rev. Sci. Instr.* **85** 013113
[18] Wernet P, Gaudin J e, Godehusen K, Schwarzkopf O and Eberhardt W 2011 *Rev. Sci. Instrum.* **82** 063114
[19] Fabris D *et al.* 2015 *Nat. Photonics* **9**(6) 383–387
[20] Cabasse A *et al.* 2013 *EPJ Web of Conferences* **41** 01015
[21] Driever S *et al.* 2014 *J. Phys. B* **47** 204013
[22] He X *et al.* 2009 *Phys. Rev. A* **79**(6) 063829
[23] Ghafur O *et al.* 2009 *Rev. Sci. Instrum.* **80** 033110
[24] Muller H G 2002 *Appl. Phys. B* **74** s17–s21
[25] Mairesse Y *et al.* 2003 *Science* **302** 1540–1543
[26] Marciniak A *et al.* 2015 *Nat. Commun. in press*
[27] Malloci G, Mulas G, Cappellini G and Joblin C 2007 *Chem. Phys.* **340** 43 – 58
[28] Dahlström J M, L'Huillier A and Maquet A 2012 *J. Phys. B* **45** 183001